JOURNAL OF MATERIALS SCIENCE **38** (2003) 1661 – 1665

Relation of microstructural and compositional features to the electrical properties in degraded thermal barrier coating systems

S.-H. SONG*
School of Materials and Metallurgy, Wuhan University of Science and Technology, Wuhan, Hubei 430081, People's Republic of China
E-mail: shenhuasong@hotmail.com

P. XIAO
Manchester Materials Science Centre, University of Manchester/UMIST, Grosvernor Street, Manchester M1 7HS, UK

Degraded thermal barrier coating samples cut from different after-service gas turbine components are examined by both electron microscopy and impedance spectroscopy. There is a relationship between the microstructural and compositional features of the thermally grown oxide (TGO) and its electrical properties. The resistance of the TGO decreases with the TGO evolution from alumina to porous mixed oxides composed probably of NiO, spinel, Cr_2O_3, and Al_2O_3, while the relaxation frequency corresponding to the TGO increases. For seriously degraded TBCs, there is an additional semicircle in the impedance spectra in the extremely low frequency range, possibly arising from cracking in the vicinity of YSZ-TGO interface regions.

1. Introduction

Thermal barrier coatings (TBCs) have widely been used on gas turbine components for increasing the gas operating temperature. A TBC system is composed of an oxidation resistant bond coat (normally, MCrAl alloy, M = Ni and/or Co) on a Ni-base superalloy substrate, a heat-insulating ceramic top coat (yittria-stablised zirconia (YSZ), $ZrO_2 + 6–8$ wt% Y_2O_3), and a thermally grown oxide (TGO) layer between the top and bond layers [1, 2]. The TGO is normally protective α-alumina. However, after long-term operation at high temperatures, this protective α-alumina would gradually evolve and degrade into a less protective mixed oxide layer [3, 4], where cracks may easily initiate and propagate, leading to the failure of TBC systems by spallation of the top coat [5, 6]. As a consequence, of concern in engineering practice is how to monitor the TGO degradation.

Owing to the fact that the electrical properties of an oxide are sensitive to its microstructure and chemical composition, we might be able to monitor the TGO degradation by monitoring the changes in its electrical properties. The aim of the present work is to evaluate microstructure, composition, and electrical properties of the TGO layer in some after-service TBC samples provided by ABB Power (Baden, Switzerland) so that a relationship among these characteristics may be obtained, which could be used to monitor the TGO degradation.

2. Experimental procedure

The TBC samples, prepared by air-plasma spraying, were cut from different after-service gas turbine components, provided by ABB Power (Baden, Switzerland). The as-received samples had three sets and were labelled S1, S2, and S3. Each set of sample was cut again into 3-4 specimens for subsequent evaluations. The nominal composition of the ceramic top coat is 92 wt% $ZrO_2 + 8$ wt% Y_2O_3, and that of the metallic bond coat is 70 wt%Ni + 21.5 wt%Cr + 8 wt%Al + 0.5 wt%Y. A J840 scanning electron microscope equipped with an energy dispersive X-ray (EDX) microanalyzer was employed to evaluate microstructure and composition of the TGO. Impedance spectroscopy was used to measure its electrical properties. For impedance measurements, the oxide layer formed at the surface of the superalloy substrate without TBCs was mechanically polished off to expose the metal, acting as one electrode. The TBC surface was cleaned in an ultrasonic bath with acetone and painted with a silver conductive paint, acting as the other electrode. The electrode area (painted area) was 64 mm^2. The silver paint was cured in air at 400°C for 30 minutes to increase the adhesion of the paint to the TBC. Impedance measurements were conducted using a Solartron SI 1255 HF frequency response analyser coupled with a Solartron 1296 Dielectric Interface, which is computer-controlled. Spectra analysis was performed by use of Zview impedance analysis software (Scribner Associates Inc, Southern Pines, NC) to

---

**Present address*: Department of Mechanical Engineering, Brunel University, Uxbridge, Middlesex UB8 3PH, UK.

0022–2461 © *2003 Kluwer Academic Publishers*

extract the electrical and dielectric properties of TBCs. In the measurements, an AC (alternating current) amplitude of 100 mV was employed and the AC frequency was in the range of 1×10^{-3} Hz to 1×10^{6} Hz. The measurements were carried out at 400°C for each set of sample. In order to acquire the temperature dependence of some properties of interest, Some measurements were also carried out at other temperatures. The mean values of the electrical properties obtained from the measurements were taken as the experimental results.

3. Results and discussion

Microstructures of the TBC for different samples are shown in Fig. 1. The TGO can clearly be seen in the sample S1. A dark oxide layer exists next to the bond coat. A grey oxide layer may be seen between the dark layer and the YSZ, but it is discontinuous in some places. Overall, the dark layer remains continuous. In addition, cracking has occurred somewhere between the YSZ and TGO. In general, the TGO have degraded to a certain extent. The TGO in the sample S2 has degraded to a much larger extent as compared with that in the sample S1. The dark layer has reduced so much and has disappeared in many places. Moreover, there is a rough and porous area (RPA) between the YSZ and the grey oxide layer. Cracking has occurred in many places between the YSZ and the RPA. The TGO in the sample S3 has fully degraded. There are almost no dark and grey layers left in the TGO and the RPA is dominant. Overall, of the three samples the extent to which the TGO degraded is the smallest for the sample S1, the largest for the sample S3. The degradation extent for the sample S2 is close to but is less than that for the sample S3.

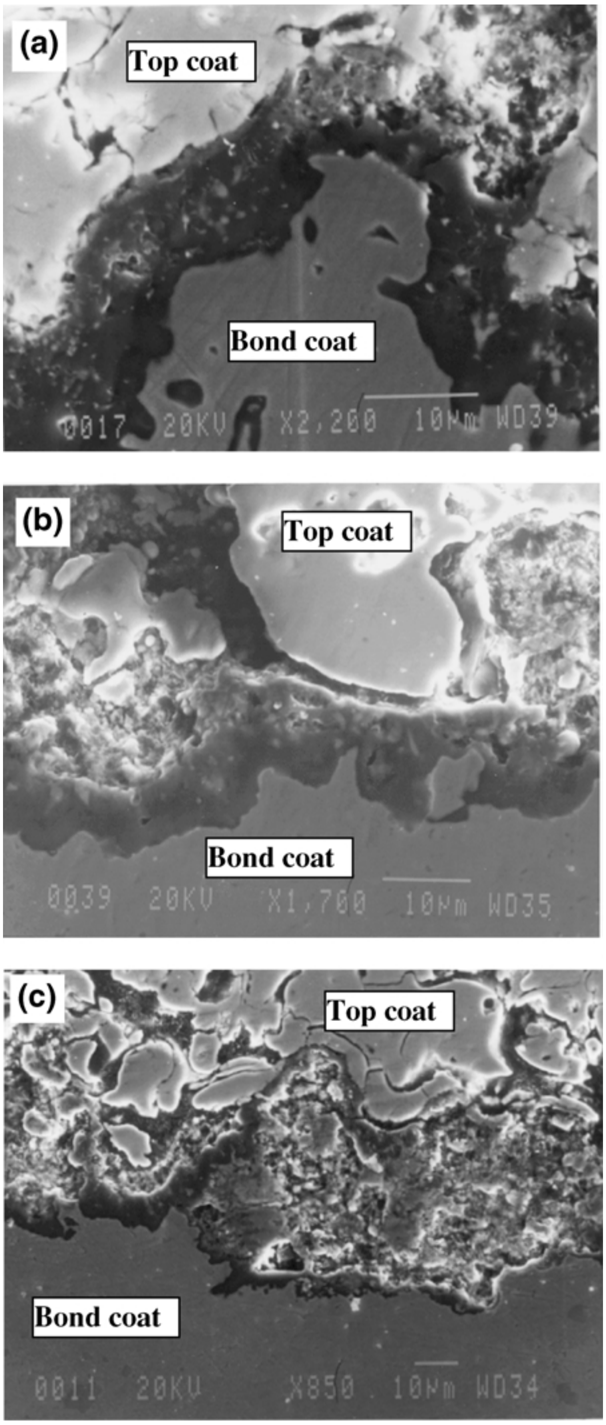

Figure 1 Scanning electron micrographs of the TBCs in the samples (a) S1, (b) S2, and (c) S3.

EDX microanalysis indicates that both dark and grey oxide layers in the sample S1 are mainly composed of alumina with an aluminium concentration over 98.5 at.%. This indicates that the grey alumina oxide originates from the evolution of the dark α-alumina and might have a different crystal structure. The concentrations of Ni, Cr, and Al in the bond coat 10 μm away from the TGO, are represented in Fig. 2 for the samples S1, S2, and S3. Owing to the fact that the aluminium content is about 8 wt% for the bond coat, the aluminium has been depleted to about 2 wt% or below, especially for the sample S3. It is the high-temperature oxidation and the formation of alumina that cause the depletion of aluminium in the bond coat. The concentrations of Ni, Cr, and Al at different positions in the grey oxide layer and the RPA are shown in Fig. 3 for the sample S2. In order to indicate the relative contents of different atoms in these two layers, the concentration in at.% has been used. Clearly, the concentrations of both Ni and Al are quite high but that of Cr is relatively small in the grey layer. This indicates that this grey layer is a mixed oxide layer containing probably alumina, spinel, NiO, and chromia but alumina and NiO are the main components. NiO and $Ni(Cr,Al)_2O_4$ spinel have also been found in the TGO elsewhere [4]. In the RPA, the concentration of Ni is apparently dominant, indicating that NiO is the

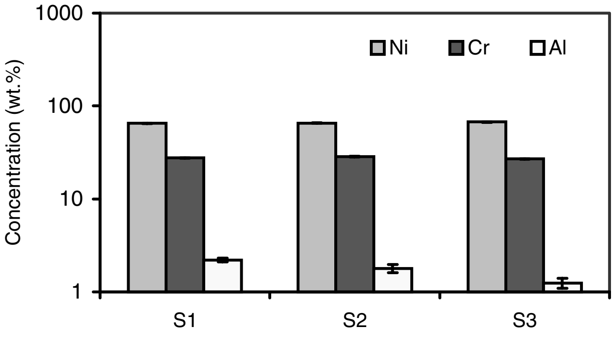

Figure 2 Concentrations of Ni, Cr, and Al in the bond coat 10 μm away from the TGO layer for different samples (Error bars represent the standard deviation).

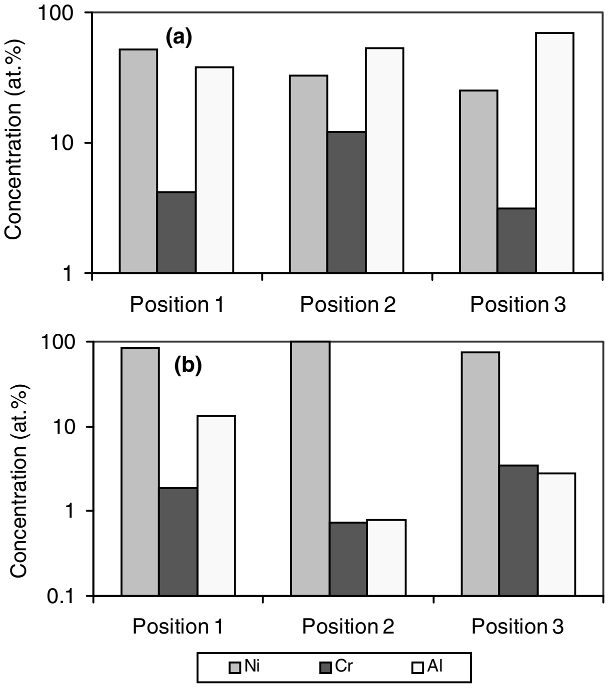

Figure 3 Concentrations of Ni, Cr, and Al at different positions (a) in the grey oxide layer and (b) in the RPA next to the top coat for the sample S2.

main component. In the light of microstructure and microchemistry, cracking may be associated with the formation of NiO because it occurs in the RPA.

In order to understand the impedance spectroscopy results, it is necessary to depict succinctly the impedance spectroscopy technique. In impedance measurements, a sinusoidal potential perturbation is applied to the test electrodes, which is contacted with the electrolyte material to be examined. Impedance diagrams are acquired by measuring the magnitude and phase shift of the resulting current. There are two types of impedance diagrams, namely Nyquist plots and Bode plots. In a Nyquist plot, the impedance is represented by a real part Z′ and an imaginary part Z″ with the formula $Z(\omega) = Z' + jZ''$, where ω is the angular frequency and $j = \sqrt{-1}$. Therefore, The Nyquist plot is also termed the complex plane impedance plot. In a Bode plot, the modulus of the impedance and the phase angle are both plotted as a function of frequency. For a simple resistor-capacitor (R-C) circuit, the Nyquist plot is characterised by a single semicircle. Usually, the Nyquist plot is used to determine the major parameters, such as resistance, capacitance and relaxation frequency corresponding to an electrochemical system. The relaxation frequency is the frequency at which the imaginary impedance is a maximum [7]. If the system is complicated, there may be several semicircles partially overlapped one another. In this scenario, the spectra have to be fitted with an equivalent circuit, which corresponds to a physical model of the system. The equivalent circuit represents the main electrical features of the model and produces a high quality of fit when fitting measured spectra [7, 8].

As described in [7, 8], for an oxide scale system, the measured capacitance response is often not ideal, i.e., not a pure capacitor. This deviation may be modified by use of a constant phase element (CPE) for spectra fitting instead of an ideal capacitance element. The impedance of a CPE is given by [7–9]

$$Z_{\mathrm{CPE}} = \frac{1}{A(j\omega)^n} \tag{1}$$

where A is a fit parameter that is independent of frequency. In the ideal case where the exponential factor $n = 1$, the CPE functions as an ideal capacitor with A equal to the capacitance C. In reality, n is less than 1. Therefore, the fitting results are represented by R, A and n. In general, the CPE behaviour may originate from some nature of oxide films or oxide-substrate interfaces, such as surface roughness or porosity, i.e., it is associated with some type of inhomogeneity, which may cause a frequency dispersion. Clearly, A value can be used to reflect the capacitance and n value to reflect the system homogeneity.

Typical Nyquist plots for different samples, obtained at 400°C, are shown in Fig. 4. Two semicircles are present for the sample S1, corresponding to two layers in the TBC. One of the two layers is the YSZ top coat and the other is the TGO layer. It has been confirmed [10–12] that the high-frequency semicircle corresponds to the YSZ top coat and the low-frequency semicircle corresponds to the TGO layer. There is an additional semicircle with some electrode effect (the linear part) at an extremely low frequency for the samples S2 and

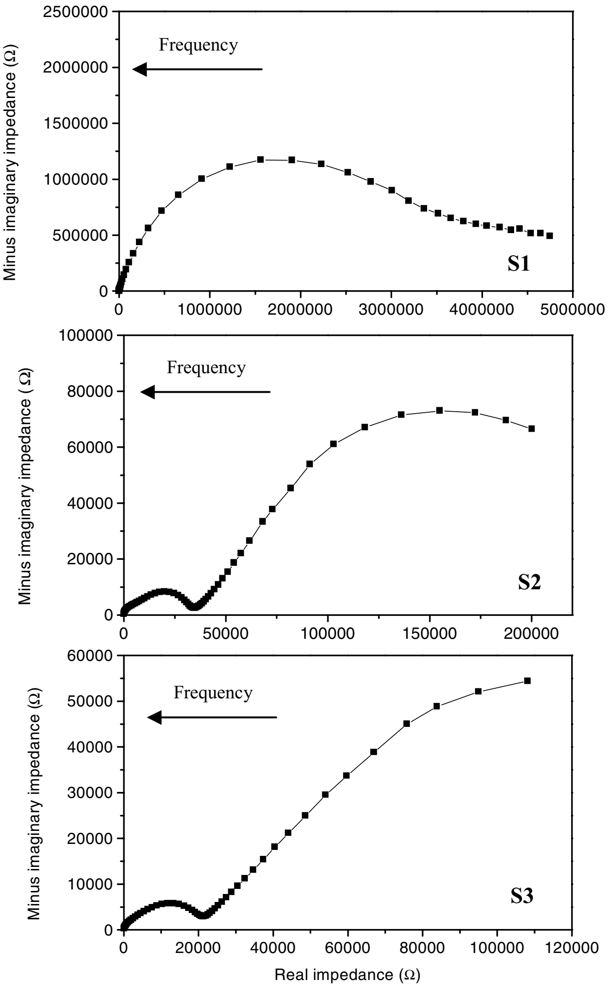

Figure 4 Typical Nyquist plots for different samples at 400°C.

S3. This semicircle might be corresponding to the interface layer between the TGO and the YSZ.

To obtain the electrical properties of the TGO layer, it is necessary to establish an equivalent circuit for fitting the measured impedance spectra. The first two semicircles (on the left-hand side) can be simulated based on a model of two R-C components with a series connection (Fig. 5a). In this equivalent circuit, CPE is the constant phase element as described above. A typical fitted impedance spectrum is shown in Fig. 5b, together with the corresponding measured one. Evidently, both fitted and measured results are well consistent. As a result, the R, A, n obtained by fitting should be close to their true values.

Fig. 6 represents the resistance and A value of the TGO layer for different samples at 400°C. The resistance for the sample S1 is of the order of 10^6 Ω but that for the two other samples is just of the order of 10^4 Ω. This demonstrates that the resistance of the TGO is very sensitive to its microstructure and composition. The A value of the TGO has no much difference (not more than one order of magnitude) between different samples, indicating its insensitive response to its microstructure and composition. This may be because the oxides contained in the TGO have no large difference in their dielectric constants. The n values corresponding to the TGO semicircles are represented in Fig. 7a for different samples. Obviously, the n value for the sample S1 is much larger than those for the two other samples, demonstrating a much more homogeneity in the sample S1 system. As expected, the relaxation frequency for the sample S1, as shown in Fig. 7b, is much lower than those for the two other samples because of its much higher resistivity. Comparing the impedance spectroscopy results with the microstructural information, we could draw the following statement. It could be possible to monitor the TGO degradation by impedance measurements. The resistance and n value decrease with the TGO degradation while the relaxation frequency increases. We also analysed the additional semicircle for the samples S2 and S3 by means of circle (arc) fitting with the analysis software mentioned above. The results are shown in Fig. 8. The resistance has no much difference for different samples and is of the order of 10^5 Ω with the value for the sample S3 somewhat lower. The capacitance is much smaller for the sample S3 than for the sample S2. Moreover, the capacitance is very large for both samples, indicating that the corresponding layer should be very thin. Allowing for the microstructural information that these two samples have degraded much more severely than the sample S1 and that the sample S3 is the worst, this additional semicircle may be attributed to the cracking in the YSZ-TGO interface regions.

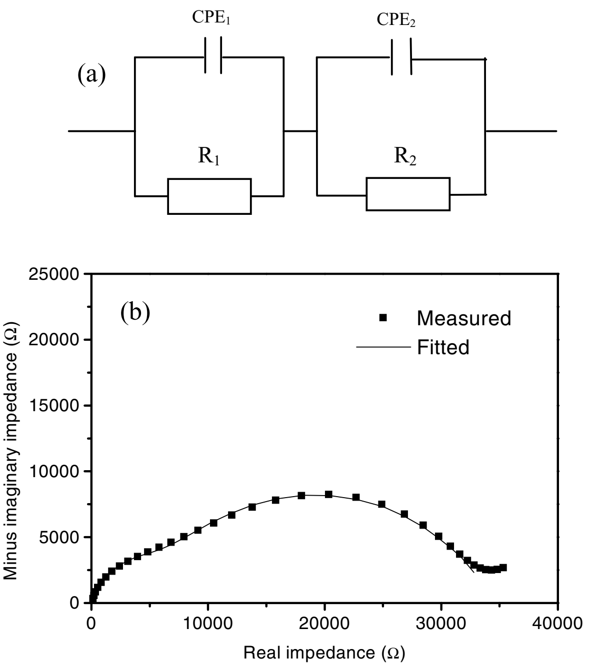

Figure 5 (a) Equivalent circuit for modelling the TBC system and (b) a typical fitted curve together with the corresponding measured impedance spectrum.

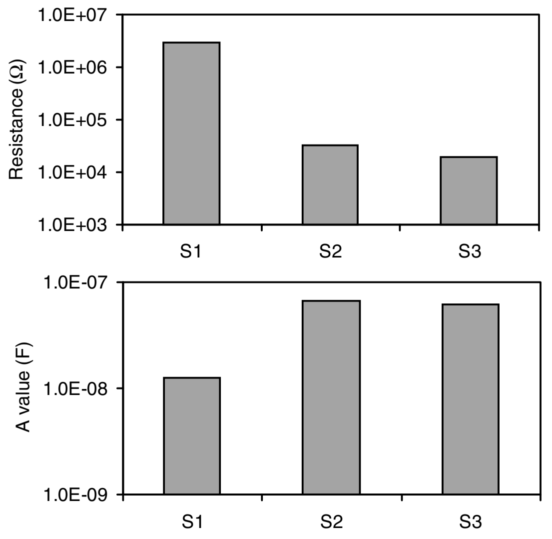

Figure 6 Resistance and A value of the TGO for different samples at 400°C.

In view of the fact that the relaxation frequency (f_R) is independent of the specimen geometry and is mainly dependent on the temperature [7], we determined its

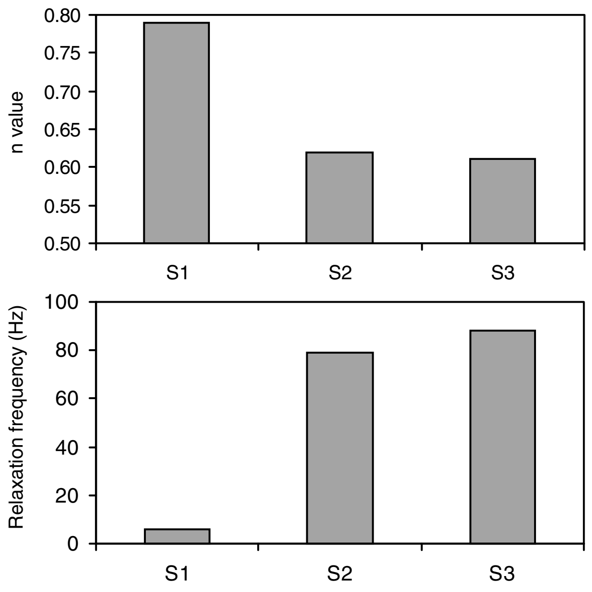

Figure 7 The n value and relaxation frequency corresponding to the TGO semicircle for different samples at 400°C.

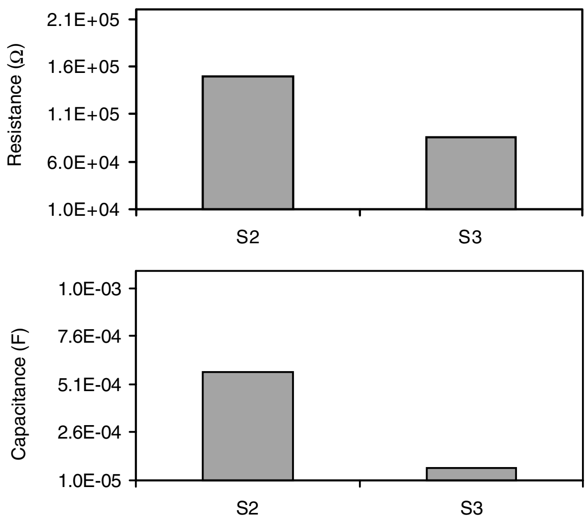

Figure 8 Resistance and capacitance corresponding to the additional third semicircle for the samples S2 and S3 at 400°C.

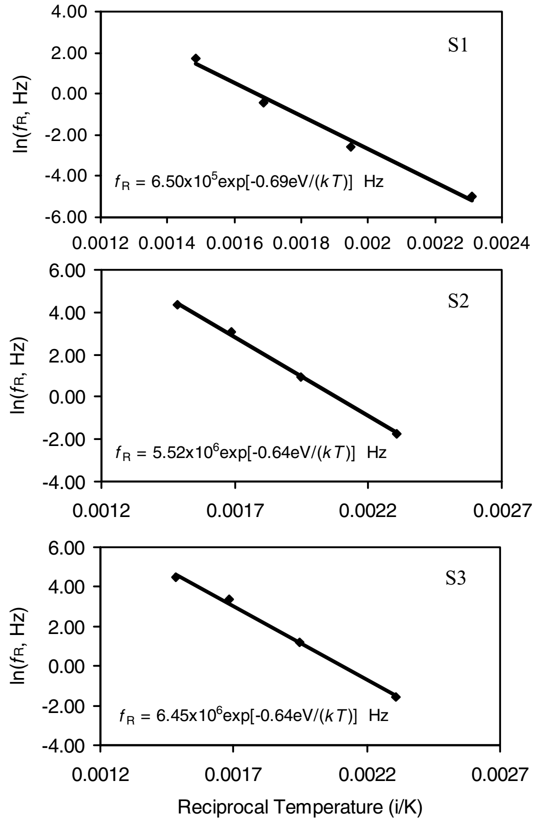

Figure 9 Relaxation frequency as a function of temperature for the TGO layer for different samples.

temperature dependence for the TGO, as shown in Fig. 9. Clearly, $\ln(f_\mathrm{R})$ has a linear relationship with the reciprocal temperature. Therefore, the relaxation frequency, f_R, may be expressed as

$$f_\mathrm{R} = f_\mathrm{Ro} \exp\left(-\frac{E_\mathrm{f}}{kT}\right) \tag{2}$$

where f_Ro and E_f are the pre-exponential constant and activation energy for relaxation, respectively, k is Boltzmann's constant, and T is the absolute temperature. Obviously, for each specimen, an activation energy, E_f, can be obtained from the slope of the line, and a pre-exponential constant, f_Ro, from the intercept of the line on the $\ln(f_\mathrm{R})$ axis. According to Fig. 9, the $f_\mathrm{R} - T$ relations for the TGO in different samples may be given by

for the sample S1

$$f_\mathrm{R} = 6.50 \times 10^5 \exp\left[-\frac{0.69\,\mathrm{eV}}{kT}\right]\mathrm{Hz} \tag{3}$$

for the sample S2

$$f_\mathrm{R} = 5.52 \times 10^6 \exp\left[-\frac{0.64\,\mathrm{eV}}{kT}\right]\mathrm{Hz} \tag{4}$$

for the sample S3

$$f_\mathrm{R} = 6.45 \times 10^6 \exp\left[-\frac{0.64\,\mathrm{eV}}{kT}\right]\mathrm{Hz} \tag{5}$$

It may be seen from Equations 3–5 that the pre-exponential constant for the sample S1 is smaller than those for the two other samples by about one order of magnitude while the activation energy is higher by 0.05 eV. This indicates a lower relaxation frequency for the sample S1 due to its higher resistivity.

4. Summary

The TBC samples from different after-service gas turbine components are evaluated by both electron microscopy and impedance spectroscopy. The results indicate that it could be possible to monitor the TGO degradation by impedance measurements. The resistance decreases with the TGO degradation while the relaxation frequency increases. For seriously degraded TBCs, there is an additional semicircle in the impedance spectra in the extremely low frequency range, which corresponds to very large capacitance and may be attributed to the cracking around the YSZ-TGO interface.

Acknowledgements

The authors would like to thank the ABB Power (Baden, Switzerland) for providing the samples.

References

1. R. L. JONES and D. MESS, *Surf. Coat. Technol.* **86/87** (1996) 94.
2. J. A. HAYNES, E. D. RIGNEY, M. K. FERBER and W. D. PORTER, *ibid.* **86/87** (1996) 102.
3. E. A. G. SHILLINGTON and D. R. CLARKE, *Acta Mater.* **47** (1999) 1297.
4. B.-C. WU, E. CHAN and S.-F. CHANG, *J. Amer. Ceram. Soc.* **72** (1989) 212.
5. M. S. ALI, S.-H. SONG and P. XIAO, *J. Mater. Sci.* **37** (2002) 2097.
6. A. H. BARTLETT and R. D. MASCHIO, *J. Amer. Ceram. Soc.* **78** (1995) 1018.
7. J. R. MACDONALD (ed.), "Impedance Spectroscopy" (John Wiley & Sons, Chichester, UK, 1987).
8. J. G. FLETCHER, A. R. WEST and J. T. S. IRVINE, *J. Electrochem. Soc.* **142** (1995) 2650.
9. S. T. AMARAL and I. L. MULLER, *Corrosion* **55** (1999) 17.
10. X. WANG, J. F. MEI and P. XIAO, *J. Mater. Sci. Lett.* **20** (2001) 47.
11. *Idem.*, *J. Euro. Ceram. Soc.* **21** (2001) 855.
12. M. S. ALI, S.-H. SONG and P. XIAO, *ibid.* **22** (2002) 101.

Received 2 July
and accepted 24 December 2002